‘Electrocatalytic Four-Electron Reduction of Dioxygen by Electrochemically Deposited Poly{[meso-tetrakis(2-thienyl)¬porphyrinato]cobalt(II)}’

ARTICLE *in* THE JOURNAL OF PHYSICAL CHEMISTRY C · MAY 2010

Impact Factor: 4.77 · DOI: 10.1021/jp101011f

Electrocatalytic Four-Electron Reduction of Dioxygen by Electrochemically Deposited Poly{[*meso*-tetrakis(2-thienyl)porphyrinato]cobalt(II)}

Wei Chen,[†] Joshua Akhigbe,[‡] Christian Brückner,[‡] Chang Ming Li,[§] and Yu Lei*[,†]

Department of Chemical, Materials and Biomolecular Engineering, University of Connecticut, Storrs, Connecticut 06269-3222, Department of Chemistry, University of Connecticut, Storrs, Connecticut 06269-3060, School of Chemical and Biomedical Engineering, Nanyang Technological University, 637457, Singapore

Received: February 2, 2010; Revised Manuscript Received: March 16, 2010

Poly{[*meso*-tetrakis(2-thienyl)porphyrinato]Co(II)} (**pCoTTP**) was deposited onto a glassy carbon electrode (GCE) through electrochemical polymerization of [*meso*-tetrakis(2-thienyl)porphyrinato]Co(II). Both cyclic voltammetry and the rotating disk electrode (RDE) techniques were employed to investigate the kinetics and mechanism of the oxygen reduction reaction (ORR) by the **pCoTTP**-modified electrode. In comparison to a bare GCE or an electrode containing the nonmetalated polymer analogue, poly[*meso*-tetrakis(2-thienyl)porphyrin] (**pTTP**), the **pCoTTP**-modified electrode shows a significant electrocatalytic enhancement of the ORR as reflected in a current increase and peak potential shift to a lower reduction potential. Koutecky−Levich plots suggest a four-electron process for oxygen reduction in acidic, neutral and basic solutions using the **pCoTTP**-modified electrode, as opposed of the two-electron process that is usually observed for monomeric cobalt porphyrins. The electrocatalytic stability of the **pCoTTP** layer and its excellent tolerance toward the poisoning by methanol is demonstrated, highlighting this electrode as a promising precious metal-free electrode material for oxygen reductions in, for instance, fuel cells.

Introduction

The increasing demand of clean energy sources drives the research on fuel cell technologies. A fuel cell is an electrochemical cell that produces electricity by the oxidation of a fuel (on the anode side) by an oxidant (on the cathode side), often oxygen.[1] Inter alia, this process requires the use of efficient electrode materials that mediate the redox processes. One obstacle for the commercialization of fuel cells is the high cost and limited availability of the most commonly used cathode material, platinum (Pt). Furthermore, Pt-based catalysts/electrodes have been found to be easily poisoned by, for instance, methanol, itself a desirable fuel. Thus over time, many Pt-based electrodes loose their activity with respect to catalyze the oxygen reduction reaction (ORR) under field conditions.[1] These problems drive the search for nonprecious metal-based, robust cathode materials that catalyze the ORR. Among a number of electrocatalysts investigated, metalloporphyrins have been identified as promising candidates.[2−5]

Conventional, monometallic metalloporphyrins catalyze the two-electron reduction of oxygen to hydrogen peroxide (eq 1).[4,6−14] However, the four-electron oxygen reduction to water is much more relevant to fuel cell applications (eq 2).

$$O_2 + 2e^- + 2H^+ \rightarrow H_2O_2 \quad (1)$$

$$O_2 + 4e^- + 4H^+ \rightarrow 2H_2O \quad (2)$$

Therefore, a number of cofacial bicobalt porphyrin structures were designed to couple two two-electron reduction events, leading to the catalysis of four-electron reduction process.[2,3,6−9] Heat-treatment (up to 1000 °C) of iron(III) tetramethoxyphenylporphyrin chloride, supported on high-area carbon, was also found to be an efficient approach to achieve a four-electron oxygen reduction.[10] Furthermore, monometallic metalloporphyrins were reported to be capable of catalyzing four-electron reduction processes when combined with carbon nanotubes[11,12] or a conducting polymer.[13]

Considering these precedents, it emerges that it is advantageous to provide the metalloporphyrin with electrons by coupling it to an electron-conductive matrix. Thus, polymerizing a suitably functionalized metalloporphyrin in a way that generates a conducting polymer appears a good means to combine the conductivity and ORR catalysis requirements. In fact, several chemically or electrochemically oligo/polymerized metalloporphyrins have been reported.[23−31] However, most of this work focused on the characterization of the electrochemical properties of the resulting polymers and not on their electrocatalytic properties. Recently, however, Lucero et al. reported the electrocatalytic oxidation of SO_3^- by polymeric iron tetra(4-aminophenyl)porphyrin.[14] Also, Chen et al. electropolymerized manganese tetra(*o*-aminophenyl)porphyrin and investigated the electrocatalytic oxidization of ascorbic acid, SO_3^{2-}, $S_2O_4^{2-}$, and Fe^{2+} in aqueous solution.[15] This group also electropolymerized iron tetra(*o*-aminophenyl)porphyrin and found the occurrence of direct four-electron reductions in ORR.[16]

meso-Thienyl-substituted porphyrins, such as *meso*-tetrakis(2-thienyl)porphyrin (**TTP**, Scheme 1) are known,[17,18] and the stronger electronic coupling of the thienyl groups to the central π-system of the porphyrin, when compared to corresponding

* Author to whom correspondence should be addressed. Fax: (+1) 860 486-2959. Telephone: (+1) 860 486-4554. E-mail: ylei@engr.uconn.edu.
[†] Department of Chemical, Materials and Biomolecular Engineering, University of Connecticut.
[‡] Department of Chemistry, University of Connecticut.
[§] Nanyang Technological University.

10.1021/jp101011f
Published on Web 04/02/2010

SCHEME 1: Synthesis of pTTP and pCoTTP

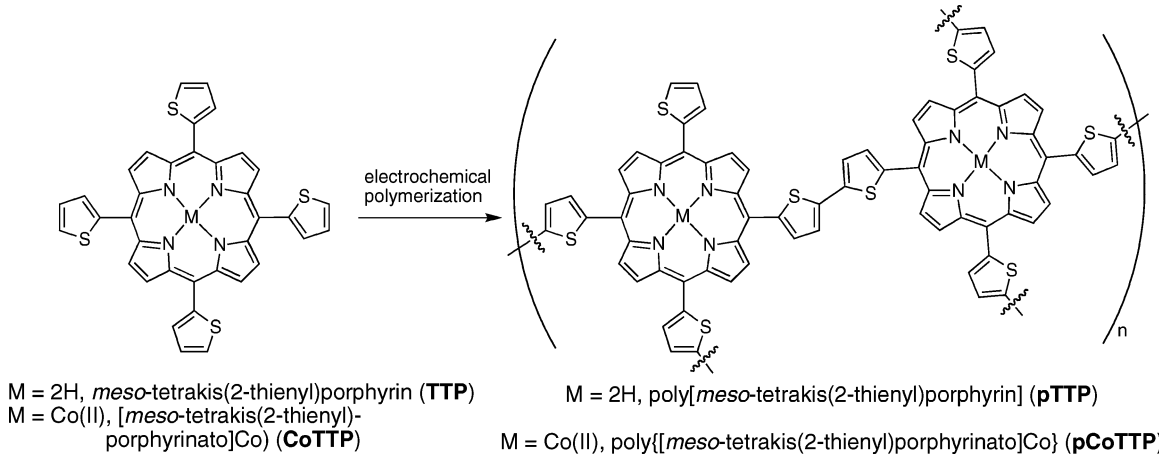

coupling of the phenyl groups in tetraphenylporphyrins, was investigated (Scheme 1).[19−23] The thienyl groups also offer the possibility to dimerize/polymerize them to obtain a heavily cross-linked polythiophene-like conducting polymer with porphyrins at its nodal points.[24−28]

We report here on the electrochemical deposition of poly{[*meso*-tetrakis(2-thienyl)porphyrinato]Co(II)} (**pCoTTP**) onto a glassy carbon electrode (GCE) and the ability of the resulting **pCoTTP**-modified electrode to catalyze the ORR. Using cyclic voltammetry and the rotating disk electrode (RDE) techniques, we investigated the electrode ORR kinetic parameters to find a four-electron reduction event. We also provide stability data and report on the resistance of the electrode toward methanol poisoning.

Experimental Methods

Materials. Sulfuric acid, sodium hydroxide, potassium hydroxide, sodium chloride, and 30% aqueous hydrogen peroxide solution were purchased from Fisher Scientific. Tetrabutylammonium hexafluorophosphate ($TBAPF_6$, 98%) and dichloromethane (anhydrous, ≥99.8%) were from Aldrich and Acros, respectively. Phosphate buffer (pH 7.0) was purchased from Sigma-Aldrich, and the pH was adjusted with 1.0 M NaOH or 0.5 M H_2SO_4. To deaerate the solutions for the electrochemical experiments, high-purity nitrogen gas (99.99%, Airgas) was bubbled through the solution for 15 min. In the oxygen reduction experiments, high-purity air (Airgas) was used to saturate the test solution with oxygen. Deionized water (17.9 MΩ-cm) was prepared using an EASYpure Barnstead system.

meso-Tetrakis(2-thienyl)porphyrin **(TTP)** was synthesized according to the Adler method as previously described.[18] [*meso*-Tetrakis(2-thienyl)porphyrinato]Co(II) **(CoTTP)** was prepared by insertion of Co(II) into **TTP** following a standard method, except that, due to the insolubility of **TTP** in acetic acid, toluene was used as the solvent.[29] Thus, **TTP** (102.4 mg, 1.60×10^{-4} mol) was dissolved in toluene (25 mL) in a round-bottom flask equipped with a magnetic stirring bar and reflux condenser. The solution was warmed, and $Co(OAc)_2 \cdot 4H_2O$ (80 mg, 3.23×10^{-4} mol, ∼2.0 equiv) dissolved in 5.0 mL of MeOH was added, and the reaction was heated to reflux. When the initial material was consumed (∼1 h, reaction controlled by UV−vis and TLC), the reaction mixture was allowed to cool to ambient temperature, and the solvent was evaporated to dryness by rotary evaporation. The residue was separated by flash column chromatography (silica−CH_2Cl_2). The major fraction was collected and recrystallized by slow solvent exchange from CH_2Cl_2 to EtOH. After air drying, **CoTTP** was isolated in 82% yield (91.0 mg) in analytical purity: R_f (silica−CH_2Cl_2) 0.90; UV−vis ($CHCl_2$) λ_{max} (log ε) 417 (5.39), 537 (4.22) nm; MS (ESI+, cone voltage = 30 V, 100% CH_3CN) *m/e* calcd for $C_{36}H_{20}N_4S_4Co$ 694.9 ($[M]^+$), found 694.6 (Micromass Quattro II).

Instruments. General electrochemical experiments were performed on a VMP3 electrochemical workstation in a conventional three-electrode cell arrangement using a glassy carbon electrode (GCE) (3.0 mm in diameter, CH Instruments) working electrode, a platinum wire counter electrode, and an Ag/AgCl, sat. KCl reference electrode. Before the electrochemical polymerizations, the GCE was successively polished with 1.0, 0.3, and 0.05 μm α-Al_2O_3 powders and sonicated in a water bath for about 5 min after each polishing step. Finally, the electrodes were rinsed thoroughly with deionized water. An ARS rotator (Pine Instrument) was employed for rotating ring-disk voltammetry in combination with an Eco Chemie Autolab bipotentiostat. A rotating glassy carbon disk-platinum ring electrode (RRDE) (5.0 mm in diameter) was used as the working electrode. Before use, the glassy carbon tip of the RRDE was put into a Teflon mount and cleaned by the same procedure as described for the GCE. UV−vis absorption spectra were recorded using a Shimadzu UV-1700 spectrophotometer. An Accumet AB15 pH meter (Fisher Scientific) was used for pH measurements. All the experiments were performed at 20 ± 1 °C.

Electrode Fabrication. The electrochemical deposition of **pCoTTP** or **pTTP** on GCE was carried out by cyclic voltammetry (CV, 0−1.5 V vs Ag/AgCl wire at a scan rate of 20 mV s^{-1}). The electrolyte consisted of 1 mM **CoTTP** or **TTP** monomer and 0.1 M $TBAPF_6$ in CH_2Cl_2. After the electropolymerization, the **pCoTTP** or **pTTP**-modified GCE was rinsed with CH_2Cl_2 to remove any nonpolymerized porphyrin residues. For the UV−vis investigation, **pCoTTP** was electrochemically deposited on a small piece of conductive ITO glass, while a **CoTTP** film was obtained by drop-deposition (from CH_2Cl_2).

Results and Discussion

TTP and its Co(II) complex, **CoTTP** (Scheme 1), were prepared using classic syntheses.[18,29] The UV−vis spectra (CH_2Cl_2) for **TTP** and **CoTTP** show the typical patterns for a free base porphyrin and metalloporphyrin, respectively (Figure 1). All spectroscopic and analytical data support the identity of **CoTTP** as the Co(II) complex of **TTP** containing a square-planar coordinated metal center and the absence of any axial ligands.

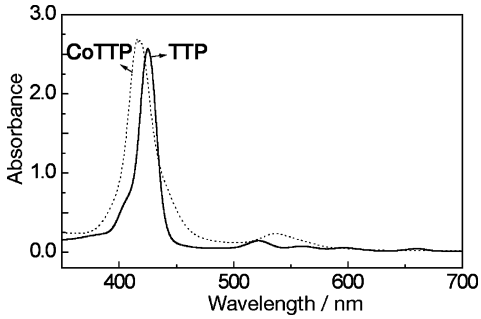

Figure 1. UV−vis spectra (CH_2Cl_2) of 10 μM of **TTP** (solid line) and **CoTTP** (dashed line).

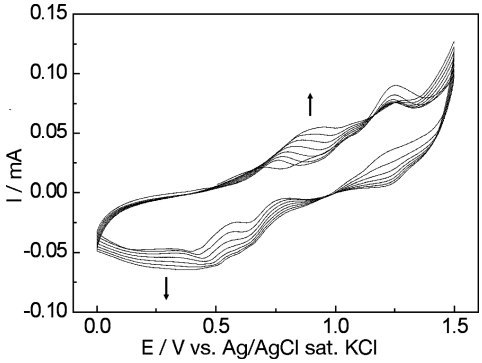

Figure 2. Repetitive cyclic voltammograms of a GCE in CH_2Cl_2 containing 1 mM **CoTTP** and 0.1 M $TBAPF_6$. Scan rate = 100 mV s^{-1}.

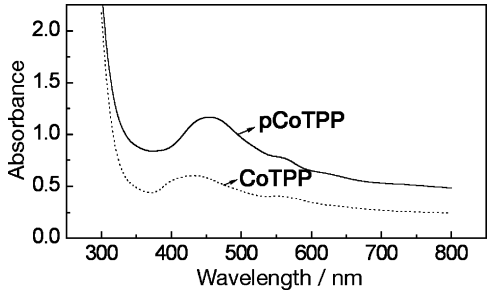

Figure 3. UV−vis spectra of **pCoTTP** (solid line) deposited by electropolymerization, and **CoTTP** (dashed line) deposited by evaporation of a CH_2Cl_2 solution onto a transparent ITO slide.

Figure 2 shows the results of repetitive CV scans of a **CoTTP** monomer solution. The currents increasing with each scan provide a clear indication for an electrochemical polymerization and growths of a **pCoTTP** conducting film on the GCE. The gradual increase of the current over 1.3 V represents the oxidation process of the thienyl groups, and its increasing value indicates that the quantity of deposited **pCoTTP** on the electrode increases over time.[26,27] In transference from the electropolymerization behavior of thiophene and related electrochemical polymerizations,[24,26−28] **CoTTP** is most likely polymerized by the electrochemical oxidative coupling of its *meso*-thienyl groups at primarily their 5-position (Scheme 1). The oxidation peak in the range of 0.7−1.0 V can be assigned to the oxidation of the porphyrin ring.[26,27]

The UV−vis spectrum of **pCoTTP** made by electropolymerization of **CoTTP** on an ITO slide is shown in Figure 3. As compared to **CoTTP** deposited on an ITO slide by drop-deposition, the Soret band of **pCoTTP** is, as a consequence of the polymerization, red-shifted by 23 nm and its half-line width ~50% broader (69 nm). This finding is consistent with the appearance of thienyl−thienyl-coupled products as *meso*-(α,α′-bis-thienyl)porphyrin and *meso*-(α,α′,α″-terthienyl)porphyrins also possess bathochromically shifted spectra as compared to **TTP**.[27] In addition, the possible presence of Co(III) porphyrins resulting from oxidation of Co(II) during the electrochemical polymerization process may also contribute to the observed shift in the optical spectra. Furthermore, exciton-coupling involving intra- or intermolecular excitonic interactions between the porphyrin subunits in the polymerized **pCoTTP** also rationalize the findings.[30−34] Exciton-coupling interactions vary with the interchromophore angles, the relative directions of the transition dipole moments in the chromophore subunits, and the distances between the chromophores; thus, the broad features of the UV−vis spectra of **pCoTTP** do not surprise.[35,36]

Figure 4 shows the CV traces of electrochemically deposited **pCoTTP** on a GCE, recorded in nitrogen-deaerated pH 7 phosphate buffer (0.01 M), NaOH (1.0 M), and H_2SO_4 (0.5 M) solutions. The **pCoTTP**-modified electrode displays three redox couples in the potential range between −0.5 and 1.0 V in pH 7 phosphate buffer solution (Figure 3a). The two couples of peaks in the range between −0.5 and 0.5 V can be assigned to the Co(II)/Co(I) and Co(III)/Co(II) metal-centered redox processes.[37] Consistent with this assignment, neither redox couple can be observed using a GCE modified with the nonmetalated analogue **pTTP** (Scheme 1, Figure 4a). The third redox couple near +0.8 V is attributed to a porphyrin ring oxidation and/or oxygen evolution peak.[38] In the CV using the **pCoTTP**-modified electrode in acidic solution (Figure 4b), the Co(III)/Co(II) reduction peak is pronounced, while the corresponding oxidation peak is very weak. Inversely, the Co(II)/Co(III) oxidation peak in basic solution can be clearly observed, but the corresponding reduction peak cannot. In addition, an irreversible anodic shoulder peak appears near +0.8 V, likely stemming from both porphyrin ring oxidation and oxygen evolution.[38]

The electrocatalytic activity of the **pCoTTP**-modified electrode for oxygen reduction was evaluated in an air-saturated pH 7.0 phosphate buffer solution (Figure 5). Oxygen reduction is indicated by the appearance of a large irreversible cathodic peak at ~−0.2 V. Besides this major peak, there are no additional reduction waves observed in the investigated potential range that might indicate the reduction of, for instance, hydrogen peroxide to water. Thus, the findings are suggestive of the reduction of oxygen to water. This reduction wave was recorded at varying scan rates, and the oxygen reduction peak currents were plotted as a function of the square root of the scan rate ($\nu^{1/2}$) (inset of Figure 5a). The resulting linear relationship confirms that oxygen reduction on the **pCoTTP**-modified electrode is, as expected, a typical diffusion-controlled electrochemical event.

A comparison of the electrocatalytic activity of the **pCoTTP**-modified GCE with a bare GCE and a free base **pTTP**-modified GCE toward oxygen reduction revealed that the oxygen reduction peak potential is lowest (by 0.3 and 0.2 V, respectively) and the peak current is highest in the **pCoTTP**-modified GCE (by 30 and 50%, respectively) (Figure 5b). Thus, the **pCoTTP** layer has a significant electrocatalytic activity with respect to oxygen reduction in neutral solution.

For an irreversible electrochemical process, the peak potential is governed by eq 3,[39]

$$E_p = E^\circ - (RT/\alpha n_\alpha F)[0.78 + \ln(D^{1/2}/k^\circ) + \ln(\alpha n_\alpha F\nu/RT)^{1/2}] \quad (3)$$

where n_α is the number of electrons involved in the rate-determining step and α is the transfer coefficient (the other

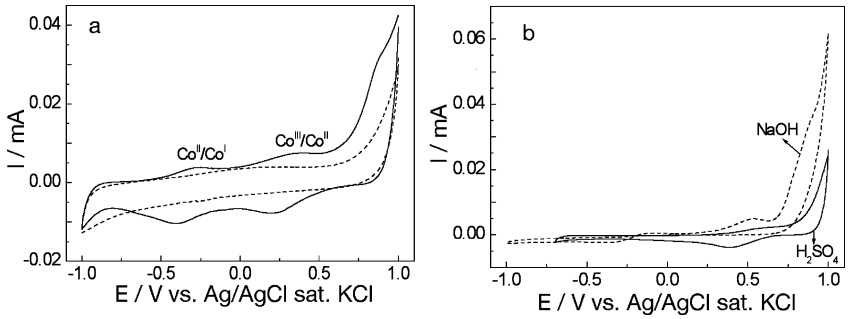

Figure 4. (a) CV traces of a **pCoTTP**-modified (solid line) and of a **pTTP**-modified (dashed line) GCE in air-saturated pH 7 phosphate buffer (0.01 M). (b) CV traces of the **pCoTTP**-modified GCE in air-saturated aqueous H_2SO_4 (0.5 M) (solid line) and NaOH (1.0 M) solutions (dashed line). Scan rate = 50 mV s^{-1}.

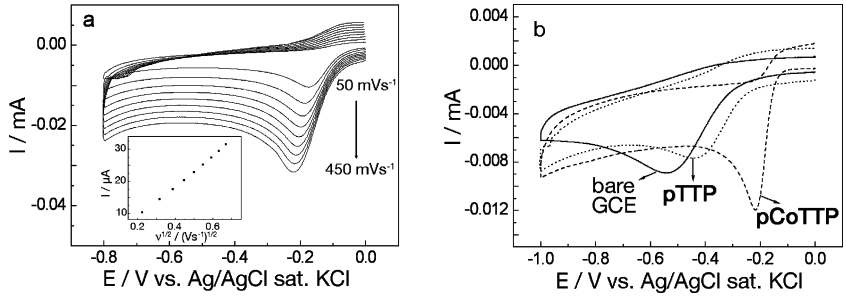

Figure 5. (a) CV traces using a **pCoTTP**-modified GCE in air-saturated pH 7.0 phosphate buffer (0.01 M) at different scan rates (50, 100, 150, 200, 250, 300, 350, 400, and 450 mV s^{-1}). Inset is the plot of peak current vs $\nu^{1/2}$. (b) CVs of the bare, **pTTP**-, and **pCoTTP**-modified GCEs in air-saturated pH 7.0 phosphate buffer (0.01 M) at a scan rate of 50 mV s^{-1}.

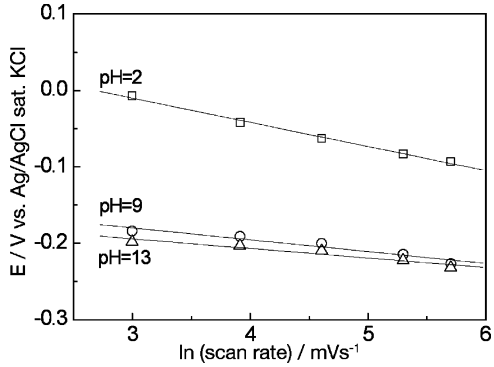

Figure 6. Plots of the peak potential of oxygen reduction (E_p) vs ln(ν) at pH 2 (□), pH 9 (○), and pH 13 (Δ).

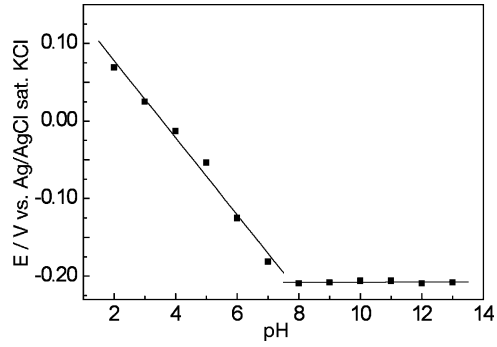

Figure 7. pH dependencies of the half-wave potential (E) of the ORR using a **pCoTTP**-modified GCE.

parameters have their usual significance). As shown in Figure 6, the plots of the oxygen reduction peak potential E_p against ln(ν) at pH values of 2, 9, and 13 show three straight lines with the slopes of 32, 15, and 12 mV/ln(ν), respectively. From these slopes, the values of αn_α were determined to be 0.39, 0.83, and 1.04, respectively. These numbers indicate that the mechanism of the electrocatalytic oxygen reduction by **pCoTTP** proceeds through a one-electron rate-determining step if assuming an α value of ~0.5 in acidic medium,[40] or it involves a two-electron rate-determining step if assuming an α value of ~1 under basic conditions.[41]

The pH dependence of the half-wave potential for oxygen reduction was also investigated (Figure 7). At pH values <7, the half-wave peak potential of oxygen reduction decreases linearly with an increase in pH values, with a slope of −50 mV/pH. Considering that the theoretical value for the slope of the potential vs pH is 59 mV p/n at room temperature (where p and n are the number of protons and electrons involved),[42] this results suggest that the oxygen reduction reaction involves the same number of protons and electrons at pH < 7. At pH values >7, the half-wave potential is pH independent.[38]

To study the kinetics of the electrocatalyzed ORR, the current−potential curves were recorded in air-saturated phosphate buffer solutions at different rotation rates and pH values using a rotating disk graphite electrode (RDE) modified with electrochemically deposited **pCoTTP**. The RDE data were analyzed using a Koutecky−Levich plot (eq 4):[39]

$$1/I_{lim} = 1/I_{Lev} + 1/I_K \quad (4)$$

Here, I_{lim} is the measured limiting current, and I_{Lev} and I_K are the Levich diffusion current and the kinetic current, respectively, described by eqs 5 and 6:

$$I_{Lev} = 0.620nFAC_O D_o^{2/3}\gamma^{-1/6}\omega^{1/2} \quad (5)$$

$$I_K = nFAK_0C_O\Gamma \quad (6)$$

In these expressions, n, D_o, and C_O are the electron number, the diffusion coefficient, and oxygen concentration, respectively,

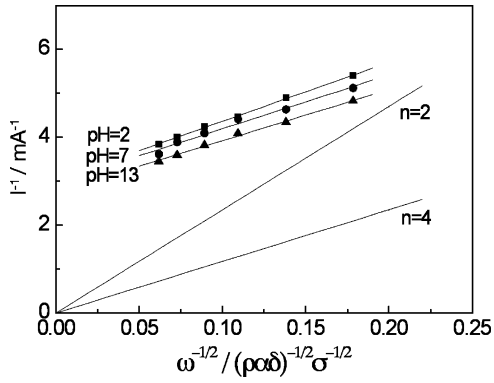

Figure 8. Koutecky−Levich plots of the plateau currents in rotating disk voltammograms for the dioxygen reduction on the **pCoTTP**-modified electrode at pH 2 (□), pH 7 (●), and pH 13 (▲). The unmarked lines are the theoretical traces for four-electron and two-electron ORR processes.

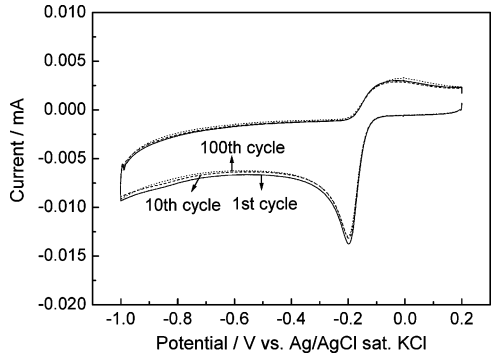

Figure 9. CVs for the ORR at the **pCoTTP**-modified electrode on the first (solid line), 10th (dashed line) and 100th (dotted line) cycles of the continuous potentiodynamic sweep in air-saturated KOH (0.1 M) at ambient temperature; scan rate = 50 mV s^{-1}.

γ the kinetic viscosity of the electrolyte solution, ω the electrode rotating rate, and K_0 is the rate constant of the chemical reaction. Figure 8 shows the corresponding Koutecky−Levich plots and the calculated graph for a two-electron and a four-electron oxygen reduction process. Clearly, the experimental data at all three pH values tested are nearly parallel to the theoretical line for a four-electron process, suggesting that dioxygen is directly reduced to water in a four-electron process. Specifically, the number of electrons involved in the ORR calculated from the slope of the experimental Koutecky−Levich plots in the pH 2, 7, and 13 buffers are 3.9, 3.82, and 4.03, respectively, all with good agreement with a four-electron oxygen reduction. The parameters used in this calculation were the following: diffusion coefficient of O_2 $D = 1.67 \times 10^{-5}$ cm^2 s^{-1}; concentration of O_2 $C_O = 1.3$ mM (pH 2), 1.1 mM (pH 7), and 1.3 mM (pH 13);[37] kinematic viscosity $\upsilon = 0.01$ cm^2 s^{-1}, $\Gamma = 5.37 \times 10^{-10}$ mol cm^{-2}; rotating disk area $A = 0.196$ cm^2. The I_K values obtained from the intercepts of the Koutecky−Levich plot are 3.02, 2.96, and 2.76 mA; and the rate constants, K_0, for pH 2, 7, and 13 are respectively 5.87×10^4, 6.93×10^4, and 5.23×10^4 M^{-1} s^{-1}, calculated from the I_K values. To further confirm the four-electron reduction of O_2, a rotating ring-disk electrode (RRDE) experiment was performed in O_2-saturated 0.01 M pH 7 phosphate buffer (Figure 1S, Supporting Information). The n value is calculated as ~3.5 from the ratio of the ring current (I_R) to the disk current (I_D) by using the following equation: $n = 4 - 2(I_R/NI_D)$.[12,13] The n value is in reasonable agreement with the result calculated from the Koutecky−Levich plot.

ORR processes catalyzed by metalloporphyrins can be classified into two-electron and four-electron mechanisms. For monomeric cobalt porphyrin, two-electron processes are generally observed.[4,6−14] Using preorganized cofacial bis(cobalt porphyrin) structures in which the cobalt centers are appropriately spaced so that dioxygen can be coordinated in a bridging mode, a four-electron process can also be realized.[2] Using the **pCoTTP**-modified electrode, a four-electron ORR process is clearly identified although no cofacial bis(cobalt porphyrin) structure was specifically designed. The thienyl group-based polymerization of **CoTTP** is believed to form a conducting network with **CoTTP** nodal points.[26] We surmise that multiple layers of these sheet- or 3D-structures are arranged such that they form suitable Co−Co bifacial binding clefts for O_2, thus allowing for facile four-electron processes.

Stability is an important factor in the performance evaluation of a catalyst. A **pCoTTP**-modified GCE was cycled 100 times between +0.2 and −1.0 V in air-saturated KOH (0.1 M), and the CV traces of the first, 10th, and 100th cycle were compared (Figure 9). The oxygen reduction peak current densities of the first, 10th, and 100th cycle were 196 mA/cm^2, 188 mA/cm^2, and 185 mA/cm^2, respectively. After the stabilization through the first 10 CV cycles, the peak current density for the 100th cycle is only 1.6% lower that that of the 10th cycle. This demonstrates the stability of the catalysts even in strongly basic solutions over a multitude of scans. In addition, the **pCoTTP**-coated electrodes are stable in water and acidic solutions (cf. to Figure 8) and organic solvents such as CH_2Cl_2.

The poisoning of, for instance, the catalysts by the fuel or fuel impurities (such as methanol) in direct alcohol fuel cells can greatly reduce their performance. Thus, the **pCoTTP**-modified GCE was subjected to testing of its poisoning tolerance (Figure 10). The strong and stable amperometric response from

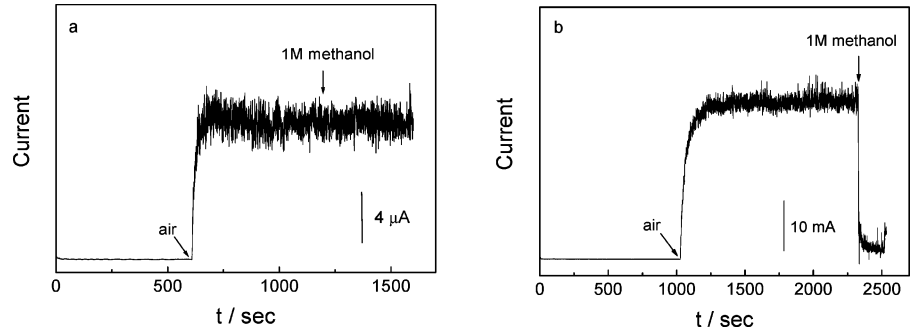

Figure 10. Chronoamperometric responses obtained at (a) the **pCoTTP**-modified GCE and (b) the commercial Pt/C-modified electrode at an applied potential of −0.25 V in KOH (0.1 M) under magnetic stirring (300 rpm) and N_2 protection, followed by introduction of air and subsequent addition of methanol (1 M).

the ORR at the **pCoTTP**-modified electrode remained unchanged even after the injection of methanol (1.0 M). As a comparison, the corresponding chronoamperometric response for a 10 μg Pt/C-modified GCE shows an immediate and sharp decrease in current upon the addition of methanol due to Pt poisoning.[43] The much lower ORR potential of the **pCoTTP**-modified GCE for the ORR than that required for oxidation of methanol likely contributes to this resistance toward MeOH poisoning.[4]

Conclusions

The electropolymerization of [*meso*-tetrakis(2-thienyl)porphyrinato]Co(II) generates a **pCoTTP**-modified GCE that showed a significant electrocatalytic activity for the four-electron oxygen reduction of dioxygen in acidic, neutral, and basic solutions, suggestive of the presence of bimetallic oxygen binding sites in the conducting polymer. The **pCoTTP**-modified electrode also has good stability for continuous potential cycling and is inert toward methanol poisoning. These features, combined with the ease of the preparation of the electrode, suggest this electrode as an attractive candidate for precious metal-free anodes in fuel cell applications.

Acknowledgment. We greatly appreciate the support of this work by the U.S. National Science Foundation under Grant No CMMI-0730826 (to Y.L. and C.B.) and CHE-0517782 (to C.B.). We also are grateful for the support from the Science and Technology Directorate of the U.S. Department of Homeland Security. "Points of view in this document are those of the author(s) and do not necessarily represent the official position of the funding agencies."

Supporting Information Available: Rotating ring-disk electrode (RRDE) voltammogram for oxygen reduction at the **pCoTTP**-modified disk electrode in O_2-saturated 0.01 M phosphate buffer (pH = 7). This material is available free of charge via the Internet at http://pubs.acs.org.

References and Notes

(1) Winter, M.; Brodd, R. J. *Chem. Rev.* **2004**, *104*, 4245.
(2) Chang, C. J.; Deng, Y. Q.; Shi, C. N.; Chang, C. K.; Anson, F. C.; Nocera, D. G. *Chem. Commun.* **2000**, 1355.
(3) Collman, J. P.; Denisevich, P.; Konai, Y.; Marrocco, M.; Koval, C.; Anson, F. C. *J. Am. Chem. Soc.* **1980**, *102*, 6027.
(4) Cui, H. F.; Ye, J. S.; Liu, X.; Zhang, W. D. *Nanotechnology* **2006**, *17*, 2334.
(5) Wang, B. J. *Power Sources* **2005**, *152*, 1.
(6) Fukuzumi, S.; Okamoto, K.; Gros, C. P.; Guilard, R. *J. Am. Chem. Soc.* **2004**, *126*, 10441.
(7) Kadish, K. M.; Fremond, L.; Ou, Z. P.; Shao, J. G.; Shi, C. N.; Anson, F. C.; Burdet, F.; Gros, C. P.; Barbe, J. M.; Guilard, R. *J. Am. Chem. Soc.* **2005**, *127*, 5625.
(8) LeMest, Y.; Inisan, C.; Laouenan, A.; Lher, M.; Talarmin, J.; ElKhalifa, M.; Saillard, J. Y. *J. Am. Chem. Soc.* **1997**, *119*, 6095.
(9) Shin, H.; Lee, D. H.; Kang, C.; Karlin, K. D. *Electrochim. Acta* **2003**, *48*, 4077.
(10) Gojkovic, S. L.; Gupta, S.; Savinell, R. F. *J. Electroanal. Chem.* **1999**, *462*, 63.
(11) Choi, A.; Jeong, H.; Kim, S.; Jo, S.; Jeon, S. *Electrochim. Acta* **2008**, *53*, 2579.
(12) Zhang, W.; Shaikh, A. U.; Tsui, E. Y.; Swager, T. M. *Chem. Mater.* **2009**, *21*, 3234.
(13) Zhou, Q.; Li, C. M.; Li, J.; Lu, J. T. *J. Phys. Chem. C* **2008**, *112*, 18578.
(14) Lucero, M.; Ramirez, G.; Riquelme, A.; Azocar, I.; Isaacs, M.; Armijo, F.; Forster, J. E.; Trollund, E.; Aguirre, M. J.; Lexa, D. *J. Mol. Catal. A: Chem.* **2004**, *221*, 71.
(15) Chen, S. M.; Chen, Y. L. *J. Electroanal. Chem.* **2004**, *573*, 277.
(16) Chen, S. M.; Chen, Y. L.; Thangamuthu, R. *J. Solid State Electrochem.* **2007**, *11*, 1441.
(17) Ono, N.; Miyagawa, H.; Ueta, T.; Ogawa, T.; Tani, H. *J. Chem. Soc., Perkin Trans.1* **1998**, 1595.
(18) Purushothaman, B.; Varghese, B.; Bhyrappa, P. *Acta Crystallogr., Sect. C: Cryst. Struct. Commun.* **2001**, *57*, 252.
(19) Collis, G. E.; Campbell, W. M.; Officer, D. L.; Burrell, A. K. *Org. Biomol. Chem* **2005**, *3*, 2075.
(20) Brückner, C.; Foss, P. C. D.; Sullivan, J. O.; Pelto, R.; Zeller, M.; Birge, R. R.; Crundwell, G. *Phys. Chem. Chem. Phys.* **2006**, *8*, 2402.
(21) Gupta, I.; Hung, C.-H.; Ravikanth, M. *Eur. J. Org. Chem.* **2003**, 4392.
(22) Bhyrappa, P.; Bhavana, P. *Chem. Phys. Lett.* **2001**, *349*, 399.
(23) Friedlein, R.; Kieseritzky, F. v.; Braun, S.; Linde, C.; Osikowicz, W.; Hellberg, J.; Salaneck, W. R. *Chem. Commun.* **2005**, *15*, 1974.
(24) Li, G.; Bhosale, S.; Tao, S.; Guo, R.; Bhosale, S.; Li, F.; Zhang, Y.; Wang, T. Y.; Fuhrhop, J.-H. *Polymer* **2005**, *46*, 5299.
(25) Odobel, F.; Suresh, S.; Blart, E.; Nicolas, Y.; Quintard, J.-P.; Janvier, P.; Le Questel, J.-Y.; Illien, B.; Rondeau, D.; Richomme, P.; Häupl, T.; Wallin, S.; Hammarström, L. *Chem.—Eur. J.* **2002**, *8*, 3027.
(26) Maruyama, H.; Segawa, H.; Sotoda, S.; Sato, T.; Kosai, N.; Sagisaka, S.; Shimidzu, T.; Tanaka, K. *Synth. Met.* **1998**, *96*, 141.
(27) Shimidzu, T.; Segawa, H.; Wu, F.; Nakayama, N. *J. Photochem. Photobiol., A* **1995**, *92*, 121.
(28) Segawa, H.; Wu, F.-P.; Nakayama, H.; Maruyama, H.; Sagisaka, S.; Higuchi, N.; Fujitsuka, M.; Shimidzu, T. *Synth. Met.* **1995**, *71*, 2151.
(29) Buchler, J. W. Synthesis and Properties of Metalloporphyrins. In *The Porphyrins*; Dolphin, D., Ed.; Academic Press: New York, 1978; Vol. 1, pp 389.
(30) Kasha, M. *Rev. Mod. Phys.* **1959**, *31*, 162.
(31) Sessler, J. L.; Capuano, V. L.; Harriman, A. *J. Am. Chem. Soc.* **1993**, *115*, 4618.
(32) Sessler, J. L.; Johnson, M. R.; Creager, S. E.; Fettinger, J. C.; Ibers, J. A. *J. Am. Chem. Soc.* **1990**, *112*, 9310.
(33) Seth, J.; Palaniappan, V.; Johnson, T. E.; Prathapan, S.; Lindsey, J. S.; Bocian, D. F. *J. Am. Chem. Soc.* **1994**, *116*, 10578.
(34) Wagner, R. W.; Lindsey, J. S. *J. Am. Chem. Soc.* **1994**, *116*, 9759.
(35) Tabushi, I.; Sasaki, T. *J. Am. Chem. Soc.* **1983**, *105*, 2901.
(36) Won, Y.; Friesner, R. A.; Johnson, M. R.; Sessler, J. L. *Photosynth. Res.* **1989**, *22*, 201.
(37) Tse, Y.; Janda, P.; Lam, H.; Zhang, J.; Pietro, W. J.; Lever, A. B. P. *J. Porphyrins Phthalocyanines* **1997**, *1*, 3.
(38) Liu, H. S.; Zhang, L.; Zhang, J. J.; Ghosh, D.; Jung, J.; Downing, B. W.; Whittemore, E. *J. Power Sources* **2006**, *161*, 743.
(39) Bard, A. J. Faulkner, L. R. *Electrochemical methods: fundamentals and applications*; John Wiley & Sons: New York, 2001.
(40) Janda, P.; Kobayashi, N.; Auburn, P. R.; Lam, H.; Leznoff, C. C.; Lever, A. B. P. *Can. J. Chem.* **1989**, *67*, 1109.
(41) van Veen, J. A. R.; Colijin, H. A. *Ber. Bunsen-Ges. Phys. Chem.* **1981**, *85*, 700.
(42) Elving, P. J. *Pure Appl. Chem.* **1963**, *7*, 423.
(43) Herrero, E.; Feliu, J. M.; Aldaz, A. *J. Electroanal. Chem.* **1994**, *368*, 101.

JP101011F